

Image Source Model of Coherent Noise in Outdoor Half-open Space

Ruan Xueyun ^{1,*}, Liu Dandan¹, Wei Haozheng ², Li Zhiyuan ² and Li Ming ³

¹ School of Mechanical Engineering, Anhui University of Science and Technology, Huainan 232001, China

² Institute of Sound & Vibration Research, Hefei University of Technology, Hefei 230009, China

³ National Center for Physical Acoustics, University of Mississippi, University, Mississippi 38677, USA

Received 8 March 2016; Accepted 13 June 2016

Abstract

Nowadays, noise prediction of industrial enterprises are mostly based on ISO 9613-2, which requires that the influence of coherent sources be disregarded. However, outdoor noise sources in industrial enterprises are mainly distributed in a half-open space and form several coherent sources because of multiple reflections. The image source model of coherent noise in outdoor half-open spaces has elicited much research attention. To increase the prediction accuracy of sound fields inside and outside half-open spaces, an image source model of noise in a half-open space was proposed. The model considers coherent sound fields. First, multi-level image sources were established through a geometric method, and the positions of image sources were determined. Second, the reflection coefficient of the plane wave and the effective sound source were determined through acoustic beam tracing. Third, analog computation of different boundary materials was implemented by adding the impedances of different boundaries. The sound fields in a half-open space with rigid impedance and absorption boundaries were calculated with the proposed, boundary element, and ISO 9613-2 models. Results showed that the ISO 9613-2 model can only reflect the overall attenuation trend of sound energy, whereas the proposed coherent image source model and the boundary element model can reflect the fluctuation trends of sound waves at different positions. The calculated results of the coherent image source model and the boundary element model were basically consistent; the errors were controlled within 1.5 dB. However, compared with the boundary element model, the proposed coherent image source model has approximately 100 times higher computational efficiency. This high accuracy reveals the proposed coherent image source model's applicability and accuracy. The model is particularly suitable for remote noise prediction in outdoor half-open spaces.

Keywords: Coherent acoustic field, Noise prediction, Half-open Space, Acoustic beam tracing

1. Introduction

The main noise sources in industrial enterprises are distributed outdoors. Plenty of sound reflections, except for diffractions, occur when sound sources are in a common half-open space formed by two finite-length vertical barriers. Currently, industrial enterprises mainly use the international mainstream prediction software to predict outdoor noises under reflections of sound sources; these software conforms to ISO 9613-2. ISO 9613-2 assumes that the sound wave is reflected once by the barrier, that is, a mirror image sound source is generated. The total sound pressure level at the receptor point can be calculated through the energy superposition of the sound pressure level after the mirror image and original sound sources have arrived at the receptor point. The algorithm assumes that energy loss during multiple reflections by the same surface is fixed. This assumption disagrees with practical situations. An image source with multiple reflections has the same frequency as the original source, and the phase difference is fixed. They are a pair of coherent sources surrounded by many coherent sound fields. Energy loss differs because of the different

angles of incidence in multiple reflections. Consequently, a large error occurs between the prediction based on energy method and the measurement. Studying the image source model of coherent noise in half-open spaces is thus necessary.

2. State of the Art

Many prediction techniques can be utilized for sound fields in closed spaces. The indoor geometric acoustic model and statistical acoustics are widely used because of their simplicity. Classical Sabine room statistical acoustic theory was proposed based on the hypothesis of the diffusion field and has been used for more than one century. However, this theory is inapplicable to half-open spaces because sound field predictions involve both indoor and outdoor fields [1], [2]. Sound field fluctuation theory is a classical, strictly accurate analytic method; however, it is only applicable to sound field prediction in closed spaces and requires a regular space shape [3], [4].

Outdoor acoustic propagation is an important problem that environmental acoustics has to solve. The noise distribution among buildings, the influences of the ground on noise propagation, the distribution of vehicle and airplane noises, and other problems can all be solved with the boundary element method[5]. In 1979, Gensane considered

* E-mail address: ruanxueyun@163.com

ISSN: 1791-2377 © 2016 Eastern Macedonia and Thrace Institute of Technology. All rights reserved.

the interferences of reflected acoustic waves and proposed an image source method that involves sound pressure interference superposition among different reflected waves; the aim was to calculate the multiple reflections of a spherical wave radiated by a point acoustic source in the space effectively [6]. Based on the ideas of Gensane et al., Lemire et al. studied point acoustic propagation in closed spaces in 1989. They believed that every reflection of the point sound source is a spherical wave. On this basis, the coherent image source model, which is widely utilized nowadays, was proposed [7]. With this theory, Dance and Wang discussed coherent image source prediction models for plant and open-plan office spaces in 1994 and 2002, respectively [8],[9]. With Lemire's coherent image source method, Chen Yan et al. from Nanjing University established a coherent model of acoustic propagation in irregular spaces in 2010 and tested the model through experiments[10]. Hequn Min from Nanjing University proposed a new coherent image source method in 2011 and used it to predict the sound field at any position in a flat conductor with one absorption ceiling and one acoustic reflected floor[11]. With the coherent image source method, Ruan Xueyun et al. from Hefei University of Technology studied the outdoor coherent noise of a converter transformer and a power transformer group in 2014[12],[13]. These studies mainly focused on sound field prediction in closed or long spaces. No research on coherent sound fields formed by multiple reflections in half-open spaces has been conducted to date. Given that Lemire's coherent image source model does not require a strictly closed space and is highly flexible, it was utilized in the present work to study an outdoor sound field in a half-open space. The image sources in the half-open space were established through a geometric method. The reflection coefficient of the plane wave was determined through acoustic beam tracing, and the contributions of different image source levels to noises at the receptor point were revealed. Finally, the total noise at the receptor point in the half-open space after multiple reflections was obtained from the coherent superposition of these contributions.

Section 2 of this paper introduces existing sound field prediction methods and elaborates the research status of sound field prediction in half-open spaces. Section 3 introduces the proposed coherent image source method for half-open spaces, constructs the geometric distribution of image sources, and proposes the use of the acoustic beam tracing method to determine the reflection coefficient of plane waves. In Section 4, sound fields in half-open spaces with rigid impedance and absorption impedance boundaries are predicted with the proposed model, the boundary element model, and the ISO 9613-2 model. Section 5 presents the conclusions.

3. Methodology

Coherent image source method, a geometric acoustic simulation method, is applicable to the prediction of sound fields in half-open spaces because of its high accuracy, simple algorithm, easy computerization, and convenient late engineering. Different from the coherent image source model for flat spaces, the coherent image source model for half-open spaces mainly predicts outdoor sound fields in half-open spaces. The following three difficulties are encountered during its establishment. First, effective image sources need to be determined according to the relative

geometric positions of the receptor point and elements of the half-open space to reduce the calculation load to the maximum extent. Second, the diffraction path has to be determined, and the diffraction field needs to be calculated when a barrier exists between the image source and the receptor point. Third, the total reflection coefficients of the image source point must be determined according to the tracked reflection paths.

3.1 Model

Given that an outdoor power transformer mainly functions between two firewalls, the sound field has a large amount of reflections, interferences, and diffractions. In this study, a coherent image source model of a power transformer in consideration of the phases was developed and used to calculate outdoor sound fields in half-open spaces. In Fig. 1, sides 1 and 2 are two firewalls. W is the distance between these two sides and H is their height. R , E_1R , and E_2R are receptor and diffraction points on left and right sides. Normalized admittance of side 1, side 2 and the ground is $\beta_i (i=1,2,3)$.

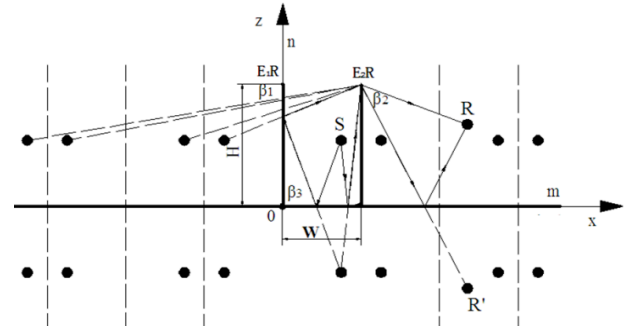


Fig.1. Structural diagram of the image source

According to the principle of image source generation, when R is on the right and outside the half-open space, the left image source ($m \leq 0$) works. Under this circumstance, the sound ray is reflected multiple times between two barriers and arrives at R through diffraction at E_2R . On the contrary, when R is on the left and outside the half-open space, the sound ray arrives at R through diffraction at E_1R . The half-open space in this study was a ground infinite rigid plane, so the diffracted sound at $E_iR (i=1,2)$ arrived at R after being reflected by the ground. The image receptor point (R') was given.

The entire sound field in the half-open space is determined by the sound source and all image sources. The image sources are generated from the continuous reflections of the sound sources at different reflection surfaces. Infinite reflections generate infinite image sources. Hence, the total sound field is determined by all image sources comprehensively. The total sound pressure at R is

$$P = \frac{A}{4\pi} \sum_{m=-\infty}^{\infty} \sum_{n=-1}^0 \sum_{i=1}^2 \sum_{j=1}^3 Q_{IS_{mn}} \left[D(IS_{mn}, R | E_{ij}) + Q_{E_{ij}} D(IS_{mn}, R' | E_{ij}) \right] \frac{e^{ikd_{E_{ij}IS_{mn}}}}{d_{E_{ij}IS_{mn}}} \quad (1)$$

where A is the strength coefficient of the point sound source; k is the wave number of the sound source; $m,n (m \in (-\infty, \infty), n \in [-1, 0])$ are the location parameters of

image sources along x,z; IS_{mn} is the exciting source or image source (hereinafter referred to as the image source); and IS_{00} is the sound source. $i(i \in [1, 2])$ represents side 1 or side 2, and $j(j \in [1, 3])$ contains the three diffraction sides (finite-length barriers). $d_{E_j IS_{mn}}$ is the distance from IS_{mn} to diffraction side E_j , Q_{E_j} is the ground reflection coefficient of the sound line after being diffracted by E_j , and $d_{E_j R}$ is the distance from IS_{mn} to $E_j R$. $D(IS_{mn}, R | E_j)$ is the single diffraction coefficient of the image sources at R through E_j , and $D(IS_{mn}, R' | E_j)$ is the single diffraction coefficient of the image sources at R' through E_j . The calculation formula of the single diffraction coefficient was introduced in Reference [14].

$Q_{IS_{mn}}$ is plural and used to calculate the total reflection coefficients of the sound wave from IS_{mn} to R . Equation (2) is the calculation formula of $Q_{IS_{mn}}$, where $Q_1(m)$ is the plural coefficient of the side passed by, and $Q_2(n)$ is the plural reflection coefficient of the ground passed by.

$$Q_{IS_{mn}} = \prod_m Q_1(m) \prod_n Q_2(n) \quad (2)$$

Lemire believed that the single reflection coefficient of reflection surfaces can be calculated from the approximate solution to the reflection field of the spherical wave on an infinite interface as follows[7]:

$$Q_i = R_{pi} + (1 - R_{pi})F(w) \quad (3)$$

where R_{pi} is the reflection coefficient of the plane wave on the i reflection surface.

$$R_{pi} = \frac{\cos \theta_{mn} - \beta_i}{\cos \theta_{mn} + \beta_i}, i = 1, 2, 3 \quad (4)$$

where θ_{mn} is incidence angle on reflection surfaces from IS_{mn} to R and β_i is the normal specific acoustic susceptance of the i surface. In Equation (3), $F(w)$ is the interface loss coefficient[15].

$$F(w) = 1 + i\sqrt{\pi}w e^{-w^2} erfc(-iw) \quad (5)$$

where $erfc$ is the complementary error function and w is the numerical distance related to m , n , θ_{mn} and the corresponding boundaries.

$$w = \sqrt{kd_{E_j IS_{mn}}} (1 + j)(\cos \theta_{mn} + \beta_i) / 2 \quad (6)$$

3.2 Determination of the reflection coefficient through acoustic beam tracing

The coherent image source method is based on the image source of specular reflection and can obtain the propagation range of the reflected sound through a geometric diagram. Although it is highly accurate, it entails calculation overload.

Theoretically, the number of image sources generated by multiple reflections is infinite; this condition leads to exponential complexity of the algorithm and explosive growth of high-order image sources. In practical situations, most image sources are not reflected at a specific receptor point, so most calculations are useless. Therefore, several acoustic ray software programs combine the image source method and the acoustic ray tracing method to simulate the sound field. An example of such a software program is ODEON, famous indoor acoustic prediction software developed in Denmark. The acoustic ray tracing method emits "acoustic particles" from a sound source to all directions and traces their propagation paths. Acoustic particles lose energies continuously upon reflection and determine new propagation directions according to the angle of incidence equal to the angle of reflection. However, the acoustic ray tracing method is disadvantageous when a large calculation load is involved because it has to produce abundant acoustic rays to prevent loss of important reflection paths. The acoustic beam tracing method is an improvement of the acoustic ray tracing method. It captures the reflection paths of the sound source on interfaces by tracing the triangular pyramidal acoustic beam. Compared with the image source method, the acoustic beam tracing method is more applicable to non-rectangular spaces and can reduce image sources more significantly. The image source method is more applicable to rectangular rooms because almost all propagation paths between the image sources and the receptor point are "visible."

Lemire's coherent image source method was utilized in this study to solve the sound field in a half-open space. Determining the plural reflection coefficient is important and involves solving the single reflection coefficient on each reflection surface. Such a single reflection coefficient is related to θ (the included angle between the acoustic ray from the image source to the receptor point and the normal of the reflection surface). This procedure requires a strict reflection path of acoustic rays. When the sound field in flat rooms (e.g., open office) is calculated with Lemire's coherent image source method, the traditional method obtains the total and single reflection coefficients by taking advantage of the relative positional relationship between every fixed image source and the receptor point. For a flat waveguide space, θ is similar to the included angle of practical reflection paths because the receptor point is in the same room; thus, the calculated result is slightly affected. However, in the studied half-open space, the receptor point is outside the space, and the calculated total reflection coefficient of a certain order of the image source based on the single reflection coefficients of previous image sources is significantly different from that obtained through actual propagation paths.

To reduce the calculation load, this study determined whether image sources in half-open spaces influence the receptor point according to the assignment of the total reflection coefficient rather than by extracting the effective sound source independently. In other words, $Q_{IS_{mn}} = 0$. Equations (1) and (2) show that the contributions of image sources to sound pressure at the receptor point are automatically defined as 0. To determine the total reflection coefficient of IS_{mn} through acoustic beam tracing method, the image sources were assumed to be reflected M times and that the receptor point was on the left of side 2. Then, $m \in [0, M]$ and $n \in [-1, 0]$. $n = 0$ means the image sources reflected by the ground are neglected, and $n = -1$ means the

image sources reflected by the ground are considered. $m = 0$ and $n = 0$ represent the image source. The reflection

paths of IS_{mn} in the half-open space determined with the acoustic beam tracing method are shown in Fig. 2 ($n = 0$).

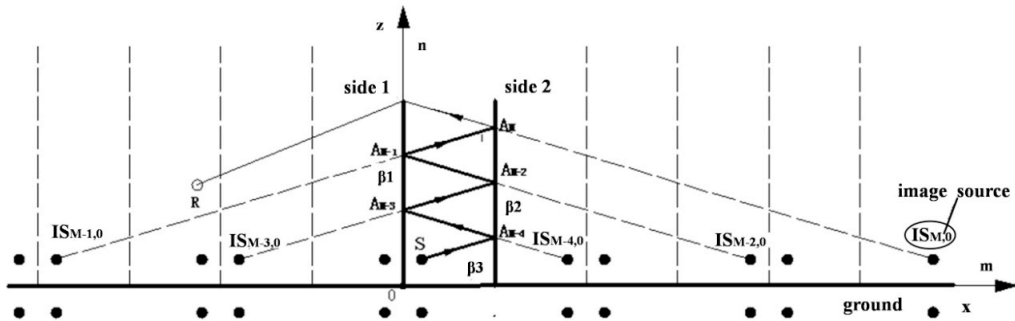


Fig.2. Reflection path in the half-open space determined with the acoustic beam tracing method ($n = 0$)

In Fig. 2, $M=5$, and the acoustic ray reflection points on sides 1 and 2 are A_i ($i \in [1, M]$). A_i is the point of intersection between the $IS_{i,0}$ - ER_i connection line and side 1 or side 2. Specifically, A_5 is the point of intersection between the $IS_{5,0}$ - ER_1 connection line and side 2, A_4 is the point of intersection between the $IS_{-4,0}$ - A_5 connection line and side 1, and A_3 is the point of intersection between the $IS_{3,0}$ - A_4 connection line and side 2. The rest can be determined in the same manner. Then, the point of intersection between A_2 and A_1 can be determined, and the reflection paths of actual acoustic rays can be described. With these reflection paths, the actual positive incident angle (θ) of each reflection can be obtained. For $IS_{5,0}$, the traced reflection paths are

$R \rightarrow A_5 (IS_{5,0}) \rightarrow A_4 (IS_{-4,0}) \rightarrow A_3 (IS_{3,0}) \rightarrow A_2 (IS_{-2,0}) \rightarrow A_1 (IS_{1,0}) \rightarrow IS_{-1,0}$. A new point of intersection is obtained by connecting every

image source to the point of intersection between the previous image source and the reflection surface. If the point of intersection is within the reflection surface, the single reflection coefficient of this reflection surface is an effective value. If one point of intersection is outside this reflection surface, the total reflection coefficient of this image source is defined as 0, and calculation module should be stopped immediately.

In the following text, the actual reflection paths of image source IS_{mn} ($n = -1$) were determined in consideration of the ground reflection. The actual incident angle can then be determined and used to calculate the single reflection coefficients accurately. The total reflection coefficient can also be determined. The reflection paths of IS_{mn} in the half-open space determined through the acoustic beam tracing method are shown in Fig. 3. The total reflections are $M = m + 1$. Considering the strict requirement of the effective image source on the ground at R , we set R in the half-open space for improved analysis.

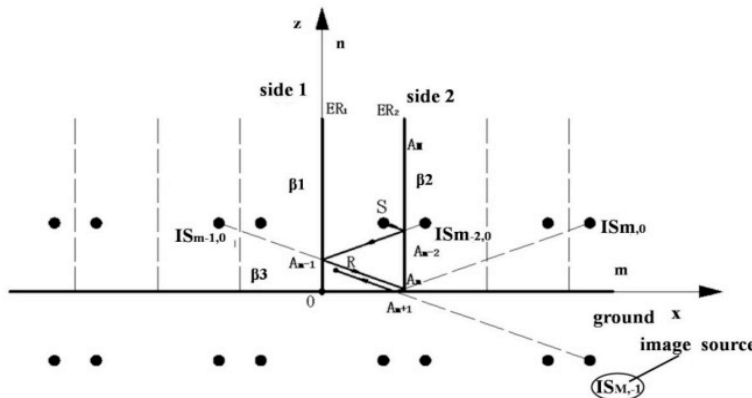


Fig.3. Reflection path in the half-open space determined with the acoustic beam tracing method ($n = -1$)

According to the principle of image source generation, the point of intersection between the R - IS_{mn} connection line and the reflection surface that generates image sources must be within the effective range of the reflection surface. Given that $n = -1$, the coherent image source model only has one ground reflection; the other reflections are on the

two parallel sides. The last ground reflection point, A_{m+1} , is the point of intersection between the R - $IS_{m,-1}$ connection line and the ground. The point of intersection between the A_{m+1} - $IS_{m,0}$ connection line and side 2 is another reflection point A_m . The other reflection points on the two sides can

be determined in the same manner by referring to the domination of reflection paths in the half-open space when $n = 0$. The traced reflection paths of $IS_{m,-1}$ are $R \rightarrow A_{m+1}(IS_{m,-1}) \rightarrow A_{m+1}(IS_{m,0}) \rightarrow A_m(IS_{-(m-1),0}) \rightarrow A_{m-1}(IS_{m-2,0}) \rightarrow L$ L $\rightarrow S$. If R and IS_{mn} are "invisible," the acoustic ray will be diffracted to R after multiple reflections by ER_1 or ER_2 . At this moment, ER_1 or ER_2 is equivalent to R . Similarly, the reflection paths were traced according to the same rules.

Fig.2 and 3 show that the actual propagation paths of the acoustic rays in the half-open space can be obtained with the acoustic beam tracing method. Hence, the single reflection coefficient of an image source can be calculated accurately. Finally, the total reflection coefficient of this image source can be obtained. The calculation flow of the total reflection coefficient ($Q_{IS_{mn}}$) of IS_{mn} at any receptor point in the half-open space based on the acoustic beam tracing method, without loss of generality, is shown in Fig. 4.

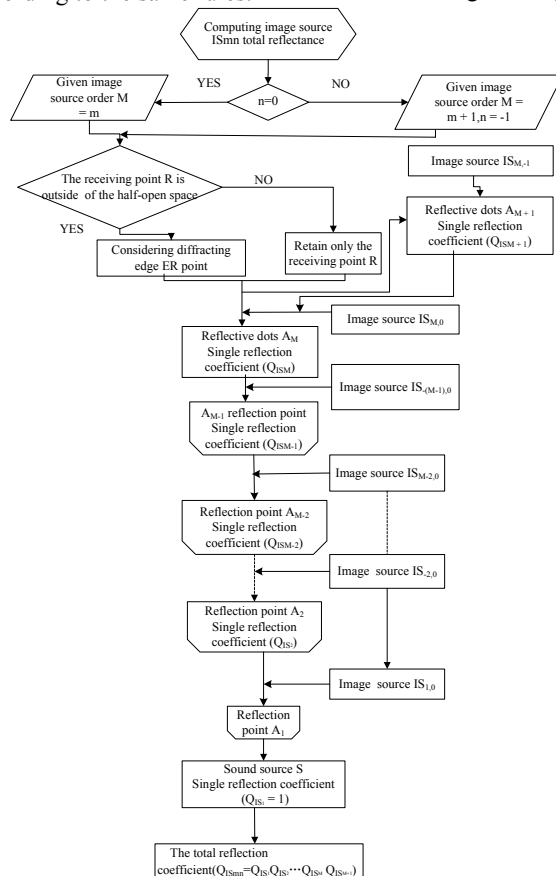


Fig.4. Reflection coefficient sequence diagram of the acoustic beam tracing method

Actual acoustic propagation paths were determined with coherent image source and acoustic beam tracing methods. The total reflection coefficient of each image source was determined from the single reflection coefficient. The sound fields in the half-open space were predicted according to Equation (1).

4. Results analysis and discussion

To verify the efficiency and accuracy of the algorithm in calculating the coherent sound field in the half-open space, a case study was conducted on 3D diffraction by a finite, long and thin barrier with a rigid ground.

4.1 Prediction of the sound field in the half-open space with a rigid impedance boundary

The sound pressure and height of point source S , which was in the middle of the two sides in the half-open space, were 1 Pa and 0.5 m respectively. The length and height of the two sides were $5\text{m} \times 2\text{m}$, and the distance between the two sides was $W = 8\text{m}$. The receptor point was 1.5m high and was in the middle of the length of two sides; it was 3m

away from side 1 horizontally. Under the assumption that the ground and two sides are rigid, the geometric size of elements in this half-open space is presented in Fig. 5.

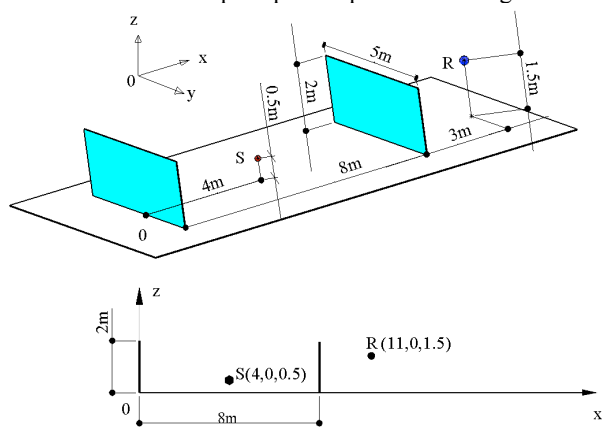


Fig.5. 3D geometric model in the half-open space

In the half-open space in Fig.5, the sound pressure when R is in the 1/3 octave band of 20Hz to 2000Hz was calculated. Given that the sound pressure of S was 1 Pa,

the source strength coefficient (A) in Equation (1) was 4π . For multiple coherent image sources, the image source with the highest order is the farthest from the receptor point. The receptor point outside the half-open space experiences minimal influence from shielding attenuation, so the sound pressure generated by this image source provides small contributions to the total sound pressure. In case 1, the reflection surfaces (ground) were defined as smooth and hard approximate rigid surfaces; flow resistance was set to $100000cgs$, $M = 15$, which can meet the accuracy requirement, was also set.

In the numerical simulation, the approximate formula of the Delany–Bazley model was utilized to assign acoustic properties of boundaries of the reflection surface. The normal specific acoustic susceptance of the interface (β) was calculated from[16]:

$$\beta = [1 + 0.057(\rho_0 f / \sigma)^{-0.754} - j0.087(\rho_0 f / \sigma)^{-0.732}]^{-1} \quad (7)$$

where $\rho_0 = 1.293 \text{ kg} \cdot \text{m}^{-3}$ is the air density at room temperature, f is the frequency of the sound source, and σ is the flow resistance of the reflection surface material, $cgs(1cgs = 1kPa \cdot s \cdot m^{-2})$. The flow resistance of common materials can be found in Reference [17]. The higher the flow resistance is, the harder the reflection surface is. According to the calculated β , the oblique incidence absorption coefficient on the interface at the angle of incidence of θ ($\alpha_\theta(f)$) and the random incidence absorption coefficient used by the interface material in the diffusion field ($\alpha_T(f)$) can be calculated as

$$\alpha_\theta(f) = 1 - \left| \frac{\cos(\theta) - \beta}{\cos(\theta) + \beta} \right| \quad (8)$$

$$\alpha_T(f) = \int_0^{\pi/2} \alpha_\theta \sin(2\theta) d\theta \quad (9)$$

Fluctuation theory can only be utilized to calculate the sound field in closed spaces; it is inapplicable to half-open spaces. To verify the accuracy of the proposed algorithm, the Virtual Lab fast multiple boundary element method was applied. The calculated results were viewed as the accurate value for comparison. The acoustic model under these software settings is shown in Fig.6. To improve computational efficiency, low and high frequencies were calculated independently. Low frequency has high wavelength and results in low meshing density. However, high frequency requires high meshing density, which costs much computation time[18].

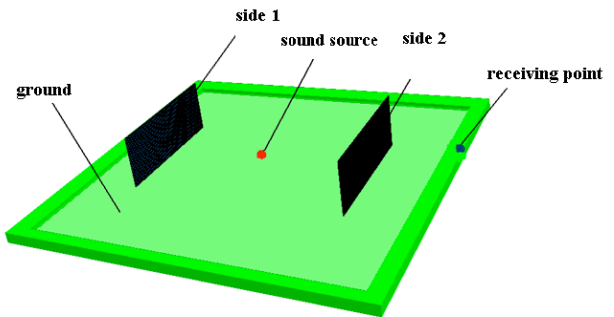


Fig.6. Half-open space geometry model based on the boundary element method

Additionally, a noise prediction software, Cadna/A, under ISO 9613-2 was used for comparative analysis with noise prediction of the ISO 9613-2 algorithm. The plane acoustic model is shown in Fig. 7. In the software settings, ground factor $G = 0$ (rigid ground), and the absorption coefficient alpha of both left and right reflection surfaces is random average absorption coefficient $\alpha_T(f)$, which can be calculated from Equations (8) and (9).

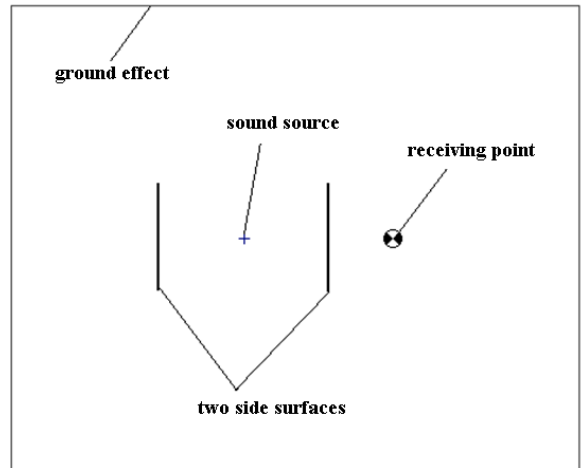


Fig.7. Half-open space geometric model based on Cadna/A

Based on the established half-open space geometric model, the frequency–sound pressure level (SPL) at R was calculated with the three methods (Fig.8). In terms of computational efficiency, the ISO 9613 model required 15s, the boundary element model required 185s, and the proposed coherent image source model required 18s.

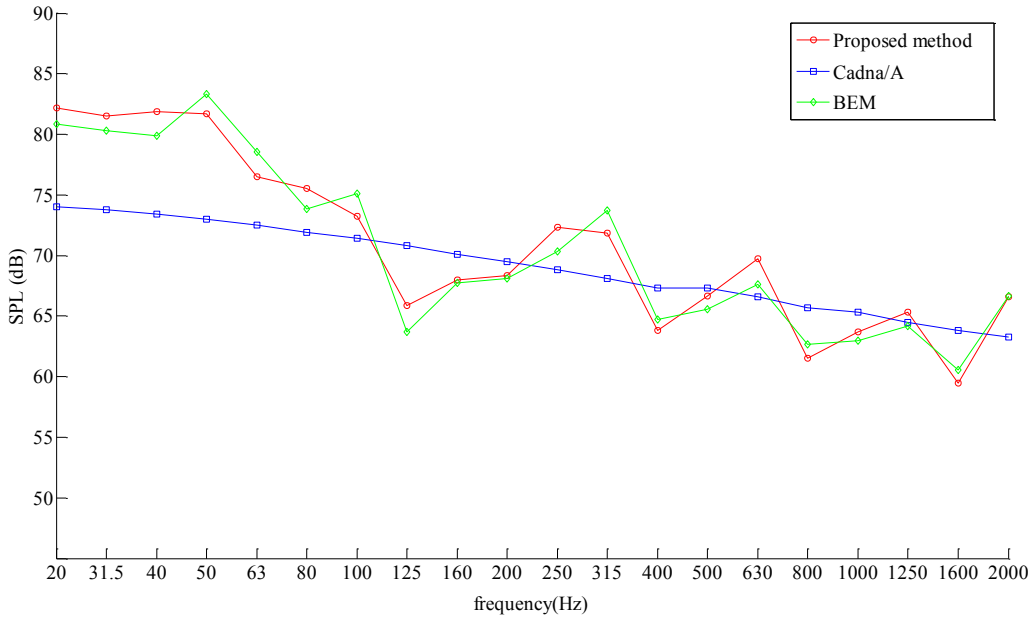


Fig.8. Spectrum results of point sound pressure level (rigid impedance boundary)

In Fig. 8, the frequency calculated by the boundary element method fluctuates with the variation of SPL, which is caused by the interference of different acoustic waves. The Cadna/A model, an incoherent prediction model based on energy method, can only reveal the variation trend of sound pressure energy and cannot predict the fluctuations caused by the interference of different reflection waves. The curve of the proposed coherent image source model is in accordance with that of the boundary element method; the average absolute error is 1.32 dB. This result indicates that the proposed model has high prediction accuracy. The proposed model consumes a similar amount of computation time as the ISO 9613 model but achieves approximately 100

times higher computational efficiency than the boundary element method.

4.2 Sound field prediction in the half-open space with absorption impedance boundaries

This case employed the same geometric model as case 1, but the two sides in this case were absorption impedance boundaries. The ground was still defined as a smooth and hard approximate rigid surface, and the flow resistance was set to $100000cgs$. Common mineral wool absorption plates were installed on the two sides, and the flow resistance was $500cgs$.

The results are shown in Fig.9.

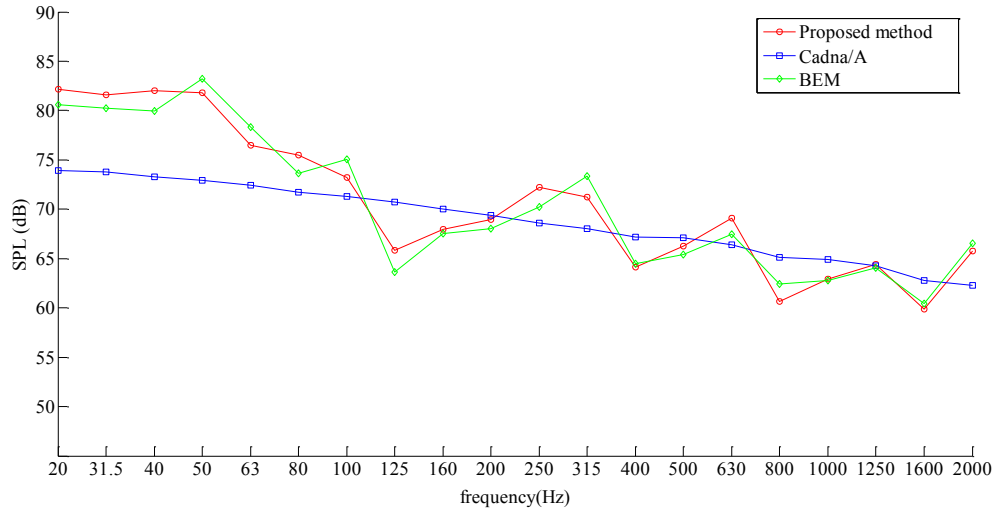


Fig.9. Spectrum results of point sound pressure level (acoustic impedance boundary)

Fig.9 shows that the prediction accuracy of Cadna/A changed slightly after the enhancement of the acoustic absorption capability of the reflection interface. Given that the receptor point is close to the sides and the barrier height is finite, the acoustic reflection at the receptor point mainly

originates from ground reflection. The side absorption materials provide small contributions to the energy of the reflected sound. Similarly, the proposed coherent image source model can not only accurately predict interferences in frequency distribution related to SPL but can also observe

the interference fluctuations of SPL at different positions. The proposed coherent image source model for half-open spaces has high prediction accuracy and computational efficiency.

5. Conclusions

To predict outdoor coherent noise in a half-open space, a coherent noise model was built for the half-open space by constructing image sources and tracing the acoustic beam through Lemire's coherent image source method. The main conclusions are shown below.

- (1) A coherent image source model of noise in a half-open space was proposed. The model can be utilized to predict the sound field inside and outside the half-open space.
- (2) The proposed calculation model can superpose the interferences of infinite image sources formed by multiple reflections. It is applicable to different boundary impedances in half-open spaces.
- (3) The sound field in the half-open space composed of rigid and absorption impedance boundaries were calculated. The results demonstrate that the current ISO 9613-2 model can

only reflect the overall distribution trend of sound field energy, whereas the proposed coherent image source model and the boundary element model can reveal the fluctuation trends of acoustic waves at different positions. The calculated results of the proposed coherent image source model and the boundary element model are basically consistent, but the proposed model has approximately 100 times higher computational efficiency than the boundary element model. This feature reveals the applicability and accuracy of the proposed model. The proposed model can be utilized to make remote noise predictions in half-open spaces.

Accurate prediction of coherent noise in half-open spaces is conducive to scientific noise management in industrial enterprises. Further investigations of the proposed coherent image source model, convergence analyses of image sources, and division of large-scaled noise sources are required.

Acknowledgements

This work was supported by Anhui Natural Science Foundation Project of China under the project No. KJ2016A201.

References

1. Lindqvist E.A.Sound., "attenuation in larger factory spaces", *Acustica*, 50(5), 1982, pp. 313-328.
2. Lam P.M., Li K.M., "A coherent model for predicting noise reduction in longenclosures with impedance discontinuities", *Journal of sound and Vibration*, 299(3), 2007, pp. 559-574.
3. Morse P.M., Ingard K.U., "Theoretical Acoustics", McGraw-Hill, New York, 1968.
4. Kuttruff H., "Room Acoustics", Applied Science Publishers Limited, London,1991.
5. TAN Jun-an., "The application of boundary element method in environment acoustics", *Noise and Vibration Control*. 41(6), 2002, pp. 20-22.
6. Gensane M, Santon F., "Prediction of sound fields inrooms of arbitrary shape: validity of the image sources method", *Journal of sound and Vibration*, 63(5), 1979, pp. 97-108.
7. Lemire G,Nicolas J., "Aerial propagation of spherical sound waves in bounded spaces", *Journal of the Acoustical Society of America*, 86(5), 1989, pp. 1845-1853.
8. Dance S M, Roberts J P, Shield B M., "Computer prediction inserton loss due to a single barrier in a non-diffuse empty enclosed spaces", *Journal of Building Acoustics*, 40(1), 1994, pp. 125-136.
9. Wang C, Bradley J S., "A mathematical model for a single screen barrier in open-plan offices", *Applied Acoustics*, 63(6), 2002, pp. 849-866.
10. Chen Yan,Liu Jianjun,Qiu Xiaojun., "Coherent model of sound propagation in the space with different long acoustic boundaries", *Journal of Nanjing University(Natural Sciences)*, 46(1), 2010, pp.26-33.
11. Min H Q., Chen Y, Qiu X J., "A coherent image source method for sound prediction in long spaces with a sound absorbent ceiling". *INTER-NOISE and NOISE-CON Congress*, Melbourne, AUSTRALIA, 2014, pp.1-9.
12. Ruan Xueyun,Li Zhiyuan,Wei Haozheng., "Research on Coherent Noise Prediction Model of Converter Transformer", *High Voltage Engineering*, 41(5), 2015, pp. 1664-1670.
13. Ruan Xueyun,Wei Haozheng,LI Zhiyuan., "Coherent prediction model of outdoor noise and its engineering application", *China Environmental Science*, 35(6), 2015, pp. 1877-1884.
14. Min H Q., Xiaojun Qiu ., "Multiple acoustic diffraction around rigid parallel wide barriers", *Journal of the Acoustical Society of America*, 126(1), 2009, pp. 179-186.
15. Muradali A, Fyfe K R., "Accurate barrier modeling in the presence of atmospheric effects", *Applied Acoustics*, 56(3), 1999, pp. 157-182.
16. Delany M.E., Bazley E.N., "Acoustical properties of fibrous absorbent materials", *Applied Acoustics*, 35(3), 1970, pp. 105-116.
17. Ma Dayou,Shen Hao., "Acoustic manual", Beijing:Science Press,China, 1983.
18. Guo Ping,Wen Guilin,Wang Yanguang et al., "Simplified algorithm of sound pressure on the three-dimensional finite noise barrier", *Journal of Highway and Transportation*, 29(8), 2012, pp. 153-158.